

Exact simulation scheme for the Ornstein–Uhlenbeck driven stochastic volatility model with the Karhunen–Loève expansions

Jaehyuk Choi^{a,*}

^a*Department of Mathematics, Columbia University*

Abstract

This study proposes a fast exact simulation scheme for the Ornstein–Uhlenbeck driven stochastic volatility model. With the Karhunen–Loève expansions, the stochastic volatility path (Ornstein–Uhlenbeck process) is expressed as a sine series, and the time integrals of volatility and variance are analytically derived as infinite series of independent normal random variables. The new method is several hundred times faster than the existing method using numerical transform inversion. The simulation variance is further reduced with conditional simulation and the control variate.

Keywords: Exact simulation, Karhunen–Loève expansions, Ornstein–Uhlenbeck process, Stochastic volatility

1. Introduction

The Ornstein–Uhlenbeck (OU) process has been widely used in quantitative finance as it balances the random walk and mean reversion. In particular, the Ornstein–Uhlenbeck driven stochastic volatility (OUSV) model [16, 18, 15] is a popular stochastic volatility model for pricing options that exhibits volatility smile. While European options can be priced with the inverse Fourier transform [15], Monte–Carlo (MC) simulation methods are required for pricing path-dependent derivatives. As such, efficient simulation has been a recent topic of research. Notably, Li and Wu [13] proposed a novel exact simulation scheme for the OUSV model, contributing to the growing literature on the exact or almost-exact simulations of stochastic volatility models [3, 1, 12, 4, 6, 8, 5]. The scheme of [13] made it possible to simulate the asset price after time step of arbitrary size without time discretization. However, the numerical Fourier transform inversion that the scheme relies on is still a computational burden, making it difficult to be widely adopted in practice. According to [13, Figures 2 and 3], their exact scheme starts to outperform the Euler discretization scheme only when the simulation time goes beyond several minutes.

This study proposes a faster exact simulation method for the OUSV model using the Karhunen–Loève (KL) expansions of the OU bridge process [9]. With the KL expansions, the stochastic volatility path can be represented as an infinite sine series where the coefficients are independent normal random variables. Therefore, it is possible to analytically obtain the time integrals of volatility and variance, which are essential components for the exact simulation. Since it avoids the costly inverse Fourier transform, the new method is several hundred times faster than [13].

The contribution of this study to the OUSV model simulation is compared to those of [10, 5] to the Heston [11] model simulation. By expressing the integrated variance under the Heston model with the infinite series of gamma random variables, [10] circumvented the computationally expensive transform inversion in the original exact simulation scheme of [3]. The gamma expansion algorithm has been further simplified by [5].

*Correspondence. *Tel:* +1-212-854-2643, *Address:* Rm 426 Mathematics Hall, 2990 Broadway, New York, NY 10027
Email address: jc6569@columbia.edu (Jaehyuk Choi)

The remainder of this paper is organized as follows. In Section 2, we introduce the OUSV model and its analytical properties. In Section 3, we express the volatility path with the KL expansions. In Section 4 and 5, we present the new simulation scheme and its numerical tests, respectively. Finally, we conclude this paper in Section 6.

2. The OUSV model and preliminaries

The stochastic differential equations for the price S_t and the stochastic volatility σ_t under the OUSV model are given by

$$\frac{dS_t}{S_t} = r dt + \sigma_t \left(\rho dZ_t + \sqrt{1 - \rho^2} dW_t \right), \quad (1)$$

$$d\sigma_t = \kappa(\theta - \sigma_t)dt + \xi dZ_t, \quad (2)$$

where W_t and Z_t are two independent standard Brownian motions, ρ is the correlation between the price and volatility, κ is the mean reversion speed, ξ is the volatility of volatility, θ is the long-term equilibrium volatility, and r is the risk-free rate.

2.1. Integrated volatility and variance

Let $U_{0,T}$ and $V_{0,T}$ be the time averages of σ_t and σ_t^2 , respectively, between $t = 0$ and T :

$$U_{0,T} = \frac{1}{T} \int_0^T \sigma_t dt \quad \text{and} \quad V_{0,T} = \frac{1}{T} \int_0^T \sigma_t^2 dt. \quad (3)$$

They are critical state variables for the OUSV model simulation because the terminal price S_T , conditional on the triplet $(\sigma_T, U_{0,T}, V_{0,T})$, follows a log-normal distribution:

$$\log(S_T/S_0) \sim N(\mu_{0,T}, \Sigma_{0,T}^2), \quad (4)$$

where the mean and variance are given by

$$\mu_{0,T} = rT + \frac{\rho}{2\xi} [(-\xi^2 - 2\kappa\theta U_{0,T} + (2\kappa - \xi/\rho) V_{0,T}) T + (\sigma_T^2 - \sigma_0^2)] \quad \text{and} \quad \Sigma_{0,T}^2 = (1 - \rho^2) T V_{0,T}.$$

See [13, Proposition 1] for the derivation. Equivalently, the asset price S_T can be expressed and simulated by a geometric Brownian motion:

$$S_T \sim F_T \exp \left(\Sigma_{0,T} Z - \frac{1}{2} \Sigma_{0,T}^2 \right) \quad (5)$$

where Z is a standard normal variable and F_T is the forward price conditional on $(\sigma_T, U_{0,T}, V_{0,T})$:

$$\begin{aligned} F_T &= E\{S_T | \sigma_T, U_{0,T}, V_{0,T}\} = S_0 \exp \left(\mu_{0,T} + \frac{1}{2} \Sigma_{0,T}^2 \right) \\ &= S_0 \exp \left(rT + \frac{\rho}{2\xi} [(-\xi^2 - 2\kappa\theta U_{0,T} + (2\kappa - \rho\xi) V_{0,T}) T + (\sigma_T^2 - \sigma_0^2)] \right). \end{aligned} \quad (6)$$

Therefore, sampling S_T is reduced to sampling σ_T , $U_{0,T}$ and $V_{0,T}$, and the challenge in the OUSV model simulation lies in sampling the triplet. In [13], σ_T and $U_{0,T}$ are sampled simultaneously as they follow a bivariate normal distribution. Then, $V_{0,T}$ is drawn from the cumulative distribution function (CDF) obtained from the inverse Fourier transform of $V_{0,T}$ for given σ_T and $U_{0,T}$. Numerical inversion requires a heavy computation. Alternatively, we will adopt the KL expansions to sample $U_{0,T}$, and $V_{0,T}$ simultaneously for given σ_T (see Section 3).

2.2. Auxiliary processes of the stochastic volatility

We define three auxiliary processes of σ_t for simulation. First, let us define $\bar{\sigma}_t$ and its time averages by removing from σ_t the long-term volatility θ :

$$\bar{\sigma}_t = \sigma_t - \theta, \quad \bar{U}_{0,T} = \frac{1}{T} \int_0^T \bar{\sigma}_t dt \quad \text{and} \quad \bar{V}_{0,T} = \frac{1}{T} \int_0^T \bar{\sigma}_t^2 dt. \quad (7)$$

Consequently, the process $\bar{\sigma}_t$ satisfies a simpler form of the OU process than Eq. (2):

$$d\bar{\sigma}_t = -\kappa\bar{\sigma}_t dt + \xi dZ_t \quad (\bar{\sigma}_0 = \sigma_0 - \theta).$$

Its solution is well-known as [17, Ch. 9]

$$\bar{\sigma}_T = \bar{\sigma}_0 e^{-\kappa T} + \xi e^{-\kappa T} \int_0^T e^{\kappa t} dZ_t.$$

The introduction of $(\bar{\sigma}_T, \bar{U}_{0,T}, \bar{V}_{0,T})$ will simplify algebra. The original triplets $(\sigma_T, U_{0,T}, V_{0,T})$ and the new triplet $(\bar{\sigma}_T, \bar{U}_{0,T}, \bar{V}_{0,T})$ are interchangeable by

$$\sigma_T = \theta + \bar{\sigma}_T, \quad U_{0,T} = \theta + \bar{U}_{0,T}, \quad \text{and} \quad V_{0,T} = \theta^2 + 2\theta\bar{U}_{0,T} + \bar{V}_{0,T}. \quad (8)$$

Second, we define the centered OU process $\hat{\sigma}_T$ by removing from $\bar{\sigma}_T$ its mean $E(\bar{\sigma}_T) = \bar{\sigma}_0 e^{-\kappa T}$,

$$\hat{\sigma}_T = \bar{\sigma}_T - \bar{\sigma}_0 e^{-\kappa T} = \xi e^{-\kappa T} \int_0^T e^{\kappa t} dZ_t \quad (\hat{\sigma}_0 = 0).$$

The centered process $\hat{\sigma}_T$ is a Gaussian process with zero mean and the covariance given by

$$\text{Cov}(\hat{\sigma}_t, \hat{\sigma}_T) = \frac{\xi^2}{2\kappa} \left(e^{-\kappa(T-t)} - e^{-\kappa(T+t)} \right) = \frac{\xi^2}{\kappa} e^{-\kappa T} \sinh(\kappa t) \quad \text{for } 0 \leq t \leq T.$$

The terminal value $\hat{\sigma}_T$ can be sampled by

$$\hat{\sigma}_T \sim \xi \sqrt{\frac{1 - e^{-2\kappa T}}{2\kappa}} Z_0 = \xi \sqrt{T\phi(2\kappa T)} Z_0 \quad \text{for a standard normal } Z_0, \quad (9)$$

where $\phi(x)$ is introduced for concise notations:

$$\phi(x) = \frac{1 - e^{-x}}{x} \quad (\phi(0) = 1).$$

The terminal value $\hat{\sigma}_T$ will be interchangeably used with σ_T or $\bar{\sigma}_T$ via $\sigma_T - \theta = \bar{\sigma}_T = \hat{\sigma}_T + \bar{\sigma}_0 e^{-\kappa T}$.

Last, we construct the OU bridge process B_t of $\hat{\sigma}_t$ ($0 \leq t \leq T$) given the terminal value $\hat{\sigma}_T$:

$$B_t = \hat{\sigma}_t - \frac{\text{Cov}(\hat{\sigma}_t, \hat{\sigma}_T)}{\text{Cov}(\hat{\sigma}_T, \hat{\sigma}_T)} \hat{\sigma}_T = \hat{\sigma}_t - \frac{\sinh(\kappa t)}{\sinh(\kappa T)} \hat{\sigma}_T \quad (B_0 = B_T = 0),$$

whose covariance follows as

$$\text{Cov}(B_s, B_t) = \text{Cov}(\hat{\sigma}_s, \hat{\sigma}_t) - \frac{\text{Cov}(\hat{\sigma}_s, \hat{\sigma}_T) \text{Cov}(\hat{\sigma}_t, \hat{\sigma}_T)}{\text{Cov}(\hat{\sigma}_T, \hat{\sigma}_T)}.$$

3. The KL expansions and its time integrals of the OU process

We will express the path of σ_t (i.e., OU process) with infinite sine series with the KL expansions. Daniluk and Muchorski [9, Theorem 2.3] has shown that the OU bridge process B_t admits the following

KL expansions:

$$B_t = \xi \sum_{n=1}^{\infty} a_n \sqrt{T} \sin\left(\frac{n\pi t}{T}\right) Z_n \quad \text{for } 0 \leq t \leq T \quad \text{and} \quad a_n = \sqrt{\frac{2}{(\kappa T)^2 + (n\pi)^2}}, \quad (10)$$

where Z_n are independent standard normal variables. The KL expansions are understood as the principal component analysis (PCA) of B_t in an ∞ -dimensional space; $\sin(n\pi t/T)$ and $a_n \sqrt{T}$ are the eigenfunctions and eigenvalues, respectively, of the covariance function, $\text{Cov}(B_s, B_t)$.

Notice that, if $\kappa = 0$ and $\xi = 1$, the centered process $\hat{\sigma}_t$ (and $\bar{\sigma}_t$) is reduced to the standard Brownian motion Z_t , and its bridge B_t to the standard Brownian bridge. Accordingly, Eq. (10) is reduced to the well-known KL expansions for the Brownian bridge [14]:

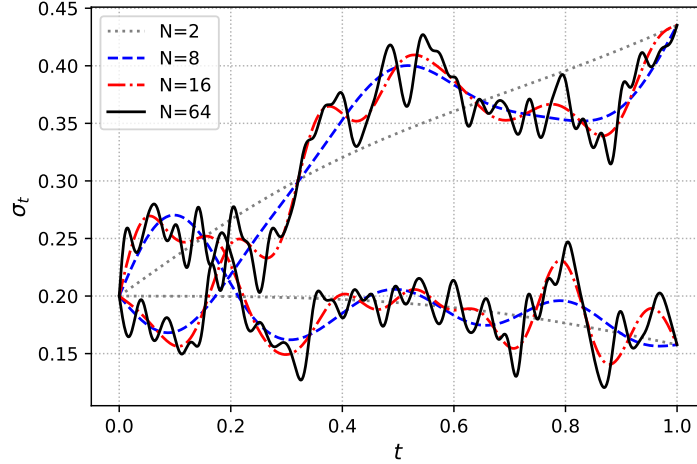
$$B_t = \sum_{n=1}^{\infty} \frac{\sqrt{2T}}{n\pi} \sin\left(\frac{n\pi t}{T}\right) Z_n \quad \text{for } 0 \leq t \leq T.$$

Using the KL expansion of B_t , the path of $\bar{\sigma}_t$, conditional on the terminal value $\hat{\sigma}_T$, is represented as follows:

$$\bar{\sigma}_t = \bar{\sigma}_0 e^{-\kappa t} + \hat{\sigma}_T \frac{\sinh(\kappa t)}{\sinh(\kappa T)} + \xi \sqrt{T} \sum_{n=1}^{\infty} a_n \sin\left(\frac{n\pi t}{T}\right) Z_n. \quad (11)$$

Figure 1 displays two example paths of σ_t represented via Eq. (11) with the terminal value σ_T fixed. As the number of sine terms increases, the paths look closer to those of the OU process.

Figure 1: Two sample volatility (OU process) paths generated by KL expansions in Eq. (11) with $N = 2, 8, 16,$ and 64 sine terms. The parameters used are $\sigma_0 = \theta = \xi = 0.2$, and $\kappa = 1$.



Since the path of $\bar{\sigma}_t$ is decomposed into elementary functions of time, it is now possible to derive

$\bar{U}_{0,T}$ and $\bar{V}_{0,T}$ in Eq. (7) analytically as infinite series of normal random variables:

$$\begin{aligned}\bar{U}_{0,T} &= \underbrace{\left[\bar{\sigma}_0 + \frac{\hat{\sigma}_T}{1 + e^{-\kappa T}} \right]}_{:=E(\bar{U}_{0,T} | \hat{\sigma}_T)} \phi(\kappa T) + 2\xi\sqrt{T} \sum_{\substack{n=1 \\ n: \text{ odd}}}^{\infty} \frac{a_n}{n\pi} Z_n, \\ \bar{V}_{0,T} &= \underbrace{\bar{\sigma}_0^2 \phi(2\kappa T) + \hat{\sigma}_T^2 \frac{\sinh(2\kappa T) - 2\kappa T}{4\kappa T \sinh^2(\kappa T)} + \frac{\xi^2}{2\kappa} \left[\coth(\kappa T) - \frac{1}{\kappa T} \right]}_{:=E(\bar{V}_{0,T} | \hat{\sigma}_T)} + \bar{\sigma}_0 \hat{\sigma}_T \frac{e^{-\kappa T}}{\kappa T} \left[\frac{1}{\phi(2\kappa T)} - 1 \right] \\ &\quad + \xi\sqrt{T} \left[\bar{\sigma}_0 \sum_{n=1}^{\infty} n\pi a_n^3 Z_n + \bar{\sigma}_T \sum_{n=1}^{\infty} (-1)^{n-1} n\pi a_n^3 Z_n \right] + \frac{\xi^2 T}{2} \sum_{n=1}^{\infty} a_n^2 (Z_n^2 - 1).\end{aligned}\quad (12)$$

See [Appendix A](#) for the detailed derivation, where the trigonometric and hyperbolic integrals are used.

In Eq. (12), we have easily identified the conditional means, $E(\bar{U}_{0,T} | \hat{\sigma}_T)$ and $E(\bar{V}_{0,T} | \hat{\sigma}_T)$, because the random variables (i.e., Z_n and $Z_n^2 - 1$) have zero means. This is an alternative derivation of [13, Eq. (7)]. From the conditional means, the unconditional means can also be obtained:

$$\begin{aligned}E(U_{0,T}) &= \theta + (\sigma_0 - \theta)\phi(\kappa T) \\ E(V_{0,T}) &= \theta^2 + \frac{\xi^2}{2\kappa} + 2\theta(\sigma_0 - \theta)\phi(\kappa T) + \left[(\sigma_0 - \theta)^2 - \frac{\xi^2}{2\kappa} \right] \phi(2\kappa T)\end{aligned}$$

Here, $E(V_{0,T})$ is the fair strike of the continuous variance swap, consistent with [15, Eq. (24)] and [2, Eq. (17)]. Therefore, we have provided an alternative derivation for the fair strike.

4. New simulation schemes based on the KL expansion

Based on the series expansion of $\bar{U}_{0,T}$ and $\bar{V}_{0,T}$ in Eq. (12), we propose a new exact simulation scheme. In the numerical implementation, we must take only finitely many terms. However, we must not simply ignore the truncated terms as the contribution of them is more important as we take less terms. Therefore, we will sample random variables from the approximated distributions of them to compensate the truncated terms.

Let an even integer L be the number of terms to take from the infinite series. The truncated terms in $\bar{U}_{0,T}$ and $\bar{V}_{0,T}$ beyond the first L terms are denoted by

$$G_L = \sum_{\substack{n=L+1 \\ n: \text{ odd}}}^{\infty} \frac{a_n}{n\pi} Z_n, \quad P_L = \sum_{\substack{n=L+1 \\ n: \text{ odd}}}^{\infty} n\pi a_n^3 Z_n, \quad Q_L = \sum_{\substack{n=L+1 \\ n: \text{ even}}}^{\infty} n\pi a_n^3 Z_n, \quad \text{and} \quad R_L = \sum_{n=L+1}^{\infty} a_n^2 (Z_n^2 - 1).$$

Let us also define several infinite series that are useful in analyzing the above terms:

$$c_L = \sum_{n=L+1}^{\infty} a_n^4, \quad f_L = \sum_{n=L+1}^{\infty} \frac{a_n^2}{(n\pi)^2}, \quad \text{and} \quad g_L = \sum_{n=L+1}^{\infty} (n\pi)^2 a_n^6. \quad (13)$$

The partial sums over the odd and even indices are denoted by single dot and double dots, respectively. For example,

$$\dot{c}_L = \sum_{\substack{n=L+1 \\ n: \text{ odd}}}^{\infty} a_n^4 \quad \text{and} \quad \ddot{c}_L = \sum_{\substack{n=L+1 \\ n: \text{ even}}}^{\infty} a_n^4. \quad (14)$$

The infinite series in Eqs. (13) and (14) admit analytic expressions (see [Appendix B](#)) and we will take advantage of them.

We first note that G_L , P_L , and Q_L follow a multivariate normal distribution with zero means and a

covariance matrix:

$$\text{Cov}(G_L, P_L, Q_L) = \begin{pmatrix} \dot{f}_L & \dot{c}_L & 0 \\ \dot{c}_L & \dot{g}_L & 0 \\ 0 & 0 & \dot{g}_L \end{pmatrix}. \quad (15)$$

Therefore, we can exactly sample G_L , P_L , and Q_L by:

$$\begin{aligned} G_L &= \sqrt{\dot{f}_L} \left(\sqrt{1 - \rho_L^2} W_1 + \rho_L W_2 \right) \quad \text{with} \quad \rho_L = \dot{c}_L / \sqrt{\dot{f}_L \dot{g}_L}, \\ P_L &= \sqrt{\dot{g}_L} W_2 \quad \text{and} \quad Q_L = \sqrt{\dot{g}_L} W_3, \end{aligned} \quad (16)$$

where W_1 , W_2 , and W_3 are standard normal random variables independent with each other and from $Z_{n \geq 0}$.

Next, we analyze R_L . The exact distribution of R_L is unknown, but the mean and variance of R_L can be obtained as

$$E(R_L) = 0 \quad \text{and} \quad \text{Var}(R_L) = 2c_L.$$

We cannot say that R_L is independent of G_L , P_L , and Q_L because they are implicitly related via $Z_{n \geq L+1}$. Nevertheless, R_L has zero correlation with G_L , P_L , and Q_L because $E(Z_i(Z_j^2 - 1)) = 0$ for all i and $j \geq L+1$. Therefore, it is reasonable to approximate R_L as

$$R_L \approx \sqrt{c_L} (W_4^2 - 1), \quad (17)$$

so that the mean and variance are matched. Here, W_4 is a normal random variable independent of W_1 , W_2 , and W_3 .

Finally, the procedure for simulating $\bar{\sigma}_T$, $\bar{U}_{0,T}$, and $\bar{V}_{0,T}$ is summarized as

$$\begin{aligned} \bar{\sigma}_T &= \bar{\sigma}_0 e^{-\kappa T} + \hat{\sigma}_T \quad \text{where} \quad \hat{\sigma}_T = \xi \sqrt{T} \phi(2\kappa T) Z_0, \\ \bar{U}_{0,T} &= E(\bar{U}_{0,T} | \hat{\sigma}_T) + 2\xi \sqrt{T} \left(\sum_{\substack{n=1 \\ n: \text{ odd}}}^L \frac{a_n}{n\pi} Z_n + G_L \right), \\ \bar{V}_{0,T} &\approx E(\bar{V}_{0,T} | \hat{\sigma}_T) + \xi \sqrt{T} \left[\bar{\sigma}_0 \left(\sum_{n=1}^L n\pi a_n^3 Z_n + P_L + Q_L \right) \right. \\ &\quad \left. + \bar{\sigma}_T \left(\sum_{n=1}^L (-1)^{n-1} n\pi a_n^3 Z_n + P_L - Q_L \right) \right] + \frac{\xi^2 T}{2} \left(\sum_{n=1}^L a_n^2 (Z_n^2 - 1) + R_L \right), \end{aligned} \quad (18)$$

where $E(\bar{U}_{0,T} | \hat{\sigma}_T)$ and $E(\bar{V}_{0,T} | \hat{\sigma}_T)$ are given in Eq. (12) and G_L , P_L , Q_L , and R_L are sampled according to Eqs. (16)–(17). Once $(\bar{\sigma}_T, \bar{U}_{0,T}, \bar{V}_{0,T})$ is obtained, they can be converted to $(\sigma_T, U_{0,T}, V_{0,T})$ by Eq. (8). Then, S_T can be sampled according to Eqs. (5)–(6).

Several comments on the new algorithm are in order. First, we expect a significant speed gain in our algorithm as it is expressed in terms of elementary functions (e.g., sinh) and standard normal variables only. Second, our algorithm contains an approximation in sampling $\bar{V}_{0,T}$ only because of R_L ; sampling $\hat{\sigma}_T$ and $\bar{U}_{0,T}$ are exact. Third, the number of terms L is the only parameter to choose in our algorithm. Whereas in [13], there are several parameters to be determined to control the error of the numerical Laplace inversion algorithm.

5. Numerical results

We numerically test the performance of the new exact simulation scheme by pricing European options, as in [13]. Since European options can be priced efficiently by the Fourier inversion [15], they are not the main target of the MC simulation in practice. Nevertheless, European option serves as a good test case to check the accuracy of the simulation schemes. The availability of a highly accurate benchmark

price is an added benefit. In the test, we use two additional techniques to minimize the MC variance: conditional MC simulation and martingale-preserving control variate. The reduced variance helps to measure the bias of the simulation scheme more accurately.

While [13] have priced options by averaging the payoff from the simulated S_T values, we instead price options by averaging the Black–Scholes prices from Eq. (5) over the simulated values of $(\sigma_T, U_{0,T}, V_{0,T})$.

$$\hat{C}_{\text{OUSV}} = e^{-rT} E_{\text{MC}} \{ C_{\text{BS}}(K, F_T, \sigma_{\text{BS}}) \} \quad \text{with} \quad \sigma_{\text{BS}} = \Sigma_{0,T}/\sqrt{T} \quad (19)$$

where E_{MC} is the MC average and $C_{\text{BS}}(K, F, \sigma_{\text{BS}})$ is the undiscounted Black–Scholes price of the call option with strike price K , forward price F , and volatility σ_{BS} . This method, often called *conditional simulation* [19], significantly reduces the MC variance because it uses the theoretical expectation over the asset price S_T . The conditional simulation is frequently adopted in the simulation studies [3, 4, 5]. For example, [4] have reported a 99% reduction in variance under the stochastic alpha-beta-rho (SABR) model.

The accuracy of option price can be further improved with the martingale-preserving control variate on F_T . The theoretical mean of the conditional forward price F_T in Eq. (6) over $(\sigma_T, U_{0,T}, V_{0,T})$ should be the unconditional forward price, $e^{rT} S_0$. However, this is not exactly observed in simulation:

$$\hat{S}_0 = e^{-rT} E_{\text{MC}} \{ F_T \} \quad (\neq S_0). \quad (20)$$

Therefore, we correct F_T by

$$F_T^{\text{cv}} = \mu F_T \quad \text{for} \quad \mu = S_0 e^{rT} / E_{\text{MC}} \{ F_T \}, \quad (21)$$

and we use F_T^{cv} instead of F_T in the Black–Scholes price, Eq. (19).

Table 1: The simulation result for $T = 1$ and other parameters in Eq. (22). “Spot Price” and “Option Price” evaluate Eqs. (20) and (19), respectively. “Option Price with CV” uses the control variate in Eq. (21). The true option price is 13.21492.

L	n_{path} (number of paths)	Spot Price		Option Price		Option Price with CV		
		Bias ($\times 10^{-4}$)	RMSE ($\times 10^{-2}$)	Bias ($\times 10^{-4}$)	RMSE ($\times 10^{-2}$)	Bias ($\times 10^{-4}$)	RMSE ($\times 10^{-2}$)	CPU Time (Seconds)
2	10,000	0.3	1.74	-0.4	4.04	-0.7	3.48	0.006
	40,000	0.3	0.87	-0.4	2.33	-0.6	1.74	0.024
	160,000	0.3	0.44	-0.4	1.17	-0.6	0.88	0.096
4	10,000	-0.2	1.73	-0.9	4.03	-0.7	3.47	0.008
	40,000	-0.2	0.87	-0.9	2.33	-0.7	1.74	0.028
	160,000	-0.2	0.44	-0.9	1.17	-0.7	0.87	0.109
6	10,000	-0.2	1.74	-0.4	4.04	-0.3	3.48	0.008
	40,000	-0.2	0.87	-0.4	2.33	-0.2	1.74	0.030
	160,000	-0.2	0.44	-0.4	1.17	-0.2	0.87	0.122

In our tests, we measure the spot price \hat{S}_0 in Eq. (20) and the option price \hat{C}_{OUSV} in Eq. (19) with or without the control variate in Eq. (21) for various KL expansion terms ($L = 2, \dots, 8$) and MC paths ($n_{\text{path}} = 1, 4, \text{ and } 16 \times 10^4$). We first generate a pool of 256×10^7 antithetic samples of $(\sigma_T, \bar{U}_{0,T}, \bar{V}_{0,T})$ and group them into $n_{\text{path}} = 1, 4, \text{ and } 16 \times 10^4$ paths, thereby creating $n_{\text{set}} = 256 \times 10^7 / n_{\text{path}}$ ($= 256, 64, \text{ and } 16 \times 10^3$) MC sets. We price \hat{S}_0 and \hat{C}_{OUSV} within each MC set and report the bias and root mean square error (RMSE) from the n_{set} results. We also measure the average CPU time for running one MC set.

For a direct comparison, we use the same parameter set in [13, Table 2]:

$$S_0 = K = 100, \quad \sigma_0 = \theta = 0.2, \quad \kappa = 4, \quad \xi = 0.1, \quad \rho = -0.7, \quad \text{and} \quad r = 0.09531. \quad (22)$$

We compute the exact option values for this parameter set with the Fourier inversion, and the prices

closely match those reported in [13].

Table 2: The simulation result for $T = 5$ and other parameters in Eq. (22). “Spot Price” and “Option Price” evaluate Eqs. (20) and (19), respectively. The true option price is 40.79769. “Option Price with CV” uses the control variate in Eq. (21).

L	n_{path} (number of paths)	Spot Price		Option Price		Option Price with CV		
		Bias ($\times 10^{-4}$)	RMSE ($\times 10^{-2}$)	Bias ($\times 10^{-4}$)	RMSE ($\times 10^{-2}$)	Bias ($\times 10^{-4}$)	RMSE ($\times 10^{-2}$)	CPU Time (Seconds)
4	10,000	19.7	9.56	10.7	12.13	-6.8	4.11	0.006
	40,000	19.7	4.78	10.7	6.35	-6.9	2.06	0.026
	160,000	19.7	2.41	10.7	3.19	-7.0	1.04	0.103
6	10,000	5.4	9.57	3.4	12.13	-1.2	4.12	0.007
	40,000	5.4	4.79	3.4	6.37	-1.4	2.06	0.028
	160,000	5.4	2.39	3.4	3.18	-1.4	1.03	0.110
8	10,000	-0.2	9.54	-1.2	12.11	-0.7	4.11	0.007
	40,000	-0.2	4.76	-1.2	6.33	-0.9	2.05	0.028
	160,000	-0.2	2.37	-1.2	3.15	-0.9	1.02	0.111

Tables 1, 2, and 3 show the results for the maturities, $T = 1, 5$ and 10 , respectively. As expected, the results become more accurate as L increases. Overall, single-digit L is enough to yield very small bias in the order of 10^{-4} . The martingale-preserving control variate on F_T further reduces both bias and RMSE simultaneously. With the control variate, the new simulation scheme produces accurate option prices even with $L = 4$. Most importantly, the new simulation method is several hundred times faster than the CPU time reported in [13]. This study implemented the simulation in Python on a personal computer running the Windows 10 operating system with an Intel Core i5-6500 (3.2 GHz) CPU and 8 GB RAM whereas [13] used Intel Core i5-4200U (2.29 GHz) CPU.

Table 3: The simulation result for $T = 10$ and other parameters in Eq. (22). “Spot Price” and “Option Price” evaluate Eqs. (20) and (19), respectively. The true option price is 62.76312. “Option Price with CV” uses the control variate in Eq. (21).

L	n_{path} (number of paths)	Spot Price		Option Price		Option Price with CV		
		Bias ($\times 10^{-4}$)	RMSE ($\times 10^{-2}$)	Bias ($\times 10^{-4}$)	RMSE ($\times 10^{-2}$)	Bias ($\times 10^{-4}$)	RMSE ($\times 10^{-2}$)	CPU Time (Seconds)
6	10,000	19.3	19.14	16.8	20.68	-1.3	2.65	0.007
	40,000	19.3	9.59	16.8	10.56	-1.6	1.33	0.028
	160,000	19.3	4.78	16.8	5.27	-1.7	0.66	0.111
8	10,000	-1.5	19.06	-1.9	20.63	0.0	2.64	0.007
	40,000	-1.5	9.50	-1.9	10.47	-0.3	1.32	0.029
	160,000	-1.5	4.73	-1.9	5.20	-0.4	0.65	0.117
10	10,000	-4.6	19.10	-4.5	20.65	0.5	2.65	0.008
	40,000	-4.6	9.57	-4.5	10.54	0.2	1.33	0.033
	160,000	-4.6	4.82	-4.5	5.31	0.1	0.67	0.132

6. Concluding remarks

This study approximates the OU process (i.e., the volatility process) with the KL expansions composed of a sine series. The KL expansions enable analytical computation of the integrals of volatility and variance, significantly speeding up the exact simulation of the OUSV model. This study is a new addition to the stream of research that applies the KL expansions to quantitative finance areas, such as volatility surface [7] and interest rate term-structure models [9]. We hope to see more applications of the KL expansion to other stochastic volatility models.

Appendix A. Integrals of trigonometric and hyperbolic functions

This appendix provides more detail on the derivation of $\bar{U}_{0,T}$ and $\bar{V}_{0,T}$ in Eq. (12) from the KL expansion, Eq. (11). The expression for $\bar{U}_{0,T}$ is obtained without difficulty based on

$$\int_0^1 \sin(n\pi x) dx = \begin{cases} 0 & \text{for even } n \\ 2/n\pi & \text{for odd } n. \end{cases}$$

The expression of $\bar{V}_{0,T}$ is first obtained as

$$\begin{aligned} \bar{V}_{0,T} = & \bar{\sigma}_0^2 \phi(2\kappa T) + \hat{\sigma}_T^2 \frac{\sinh(2\kappa T) - 2\kappa T}{4\kappa T \sinh^2(\kappa T)} + \frac{\xi^2 T}{2} \sum_{n=1}^{\infty} a_n^2 Z_n^2 + \bar{\sigma}_0 \hat{\sigma}_T \frac{e^{-\kappa T}}{\kappa T} \left(\frac{1}{\phi(2\kappa T)} - 1 \right) \\ & + \bar{\sigma}_0 \xi \sqrt{T} \sum_{n=1}^{\infty} (1 + (-1)^{n-1} e^{-\kappa T}) n\pi a_n^3 Z_n + \hat{\sigma}_T \xi \sqrt{T} \sum_{n=1}^{\infty} (-1)^{n-1} n\pi a_n^3 Z_n. \end{aligned} \quad (\text{A.1})$$

The six terms above are obtained in the order of

$$\int_0^T dt (A + B + C)^2 = \int_0^T dt (A^2 + B^2 + C^2 + 2AB + 2AC + 2BC),$$

where A , B , and C are the three terms of $\bar{\sigma}_t$ in Eq. (11):

$$A := \bar{\sigma}_0 e^{-\kappa t}, \quad B := \hat{\sigma}_T \frac{\sinh(\kappa t)}{\sinh(\kappa T)}, \quad \text{and} \quad C := \xi \sqrt{T} \sum_{n=1}^{\infty} a_n \sin\left(\frac{n\pi t}{T}\right) Z_n.$$

In the integrals of C^2 , AC , and BC , the following integrals of the trigonometric and hyperbolic functions have been used respectively:

$$\begin{aligned} \int_0^1 \sin(m\pi x) \sin(n\pi x) dx &= \frac{1}{2} \delta_{mn}, \\ \int_0^1 e^{-\lambda x} \sin(n\pi x) dx &= \frac{n\pi}{\lambda^2 + (n\pi)^2} (1 + (-1)^{n-1} e^{-\lambda}), \\ \int_0^1 \sinh(\lambda x) \sin(n\pi x) dx &= \frac{(-1)^{n-1} n\pi}{\lambda^2 + (n\pi)^2} \sinh(\lambda). \end{aligned}$$

where m and n are integer values, and δ_{mn} is the Kronecker delta.

Using the analytic expressions of infinite series,

$$b_0(\lambda) = \sum_{n=1}^{\infty} \frac{2}{\lambda^2 + (n\pi)^2} = \frac{\lambda \coth(\lambda) - 1}{\lambda^2} \left(\frac{1}{3} \quad \text{if } \lambda = 0 \right), \quad (\text{A.2})$$

we can re-express the third term of (A.1) with $\lambda = \kappa T$:

$$\sum_{n=1}^{\infty} a_n^2 Z_n^2 = \sum_{n=1}^{\infty} a_n^2 (Z_n^2 - 1) + \frac{\kappa T \coth(\kappa T) - 1}{(\kappa T)^2}.$$

After simplifying the last two terms with $\bar{\sigma}_T = \bar{\sigma}_0 e^{-\kappa T} + \hat{\sigma}_T$, we obtain the expression of $\bar{V}_{0,T}$ presented in Eq. (12).

In the derivation of $\bar{U}_{0,T}$ and $\bar{V}_{0,T}$ above, we exchanged the order of the infinite sum and integral. This is possible because the KL theorem [14] states that, given a path of B_t ($0 \leq t \leq T$), the convergence of the KL expansion in Eq. (10) to the path is uniform in t .

Appendix B. Analytic solutions of infinite series

The infinite sums in Eqs. (13) can be evaluated analytically. For convenience, we re-define a_n as a function of $\lambda = \kappa T$:

$$a_n = \sqrt{\frac{2}{\lambda^2 + (n\pi)^2}}.$$

Therefore, c_L , f_L , and g_L in Eq. (13) are also understood as functions of $\lambda = \kappa T$. In addition to the infinite sums in Eq. (13), we extend the definition of $b_0(\lambda)$ in Eq. (A.2) and define $d_L(\lambda)$ to be used below:

$$b_L(\lambda) = \sum_{n=L+1}^{\infty} a_n^2 \quad \text{and} \quad d_L(\lambda) = \sum_{n=L+1}^{\infty} a_n^6.$$

The infinite sums, $c_0(\lambda)$ and $d_0(\lambda)$ (i.e., $L = 0$), are sequentially derived as the derivatives with respect to λ :

$$c_0(\lambda) = \sum_{n=1}^{\infty} \frac{4}{(\lambda^2 + (n\pi)^2)^2} = -\frac{1}{\lambda} \frac{\partial}{\partial \lambda} b_0(\lambda) = \frac{1}{\lambda^4} \left(\frac{\lambda}{\tanh(\lambda)} + \frac{\lambda^2}{\sinh(\lambda)^2} - 2 \right),$$

$$d_0(\lambda) = \sum_{n=1}^{\infty} \frac{8}{(\lambda^2 + (n\pi)^2)^3} = -\frac{1}{2\lambda} \frac{\partial}{\partial \lambda} c_0(\lambda) = \frac{1}{2\lambda^6} \left(\frac{3\lambda}{\tanh(\lambda)} + \frac{\lambda^2(3 + 2\lambda/\tanh(\lambda))}{\sinh(\lambda)^2} - 8 \right).$$

Here, we interchanged the differentiation and summation because the convergence of $b_0(\lambda)$ and $c_0(\lambda)$ are uniform in $\lambda \geq 0$.

The infinite sums, $f_0(\lambda)$ and $g_0(\lambda)$, are derived as the differences:

$$f_0(\lambda) = \sum_{n=1}^{\infty} \frac{2}{(n\pi)^2(\lambda^2 + (n\pi)^2)} = \frac{1}{\lambda^2} \sum_{n=1}^{\infty} \left[\frac{2}{(n\pi)^2} - \frac{2}{\lambda^2 + (n\pi)^2} \right] = \frac{b_0(0) - b_0(\lambda)}{\lambda^2},$$

$$g_0(\lambda) = \sum_{n=1}^{\infty} \frac{8(n\pi)^2}{(\lambda^2 + (n\pi)^2)^3} = \sum_{n=1}^{\infty} \left[\frac{8}{(\lambda^2 + (n\pi)^2)^2} - \frac{8\lambda^2}{(\lambda^2 + (n\pi)^2)^3} \right] = 2c_0(\lambda) - \lambda^2 d_0(\lambda).$$

The sums of the even- and odd-indexed terms in c_0 , d_0 , and f_0 can also be derived. For example, the even-indexed sum in c_0 is given by

$$\ddot{c}_0(\lambda) = \sum_{\substack{n=1 \\ n: \text{even}}}^{\infty} \frac{4}{(\lambda^2 + (n\pi)^2)^2} = \sum_{n=1}^{\infty} \frac{4}{(\lambda^2 + (2n\pi)^2)^2} = \frac{1}{2^4} \sum_{n=1}^{\infty} \frac{4}{((\lambda/2)^2 + (n\pi)^2)^2} = \frac{c_0(\lambda/2)}{16}.$$

The similar trick applies to $f_0(\lambda)$ and $g_0(\lambda)$:

$$\ddot{f}_0(\lambda) = \frac{f_0(\lambda/2)}{16} \quad \text{and} \quad \ddot{g}_0(\lambda) = \frac{g_0(\lambda/2)}{16}.$$

Then, the sums of the odd-indexed terms follow as

$$\dot{c}_0(\lambda) = c_0(\lambda) - \ddot{c}_0(\lambda) = c_0(\lambda) - \frac{c_0(\lambda/2)}{16},$$

$$\dot{f}_0(\lambda) = f_0(\lambda) - \frac{f_0(\lambda/2)}{16}, \quad \text{and} \quad \dot{g}_0(\lambda) = g_0(\lambda) - \frac{g_0(\lambda/2)}{16}.$$

Finally, the sums for $L > 0$ are obtained by subtracting the first L terms. For example,

$$c_L(\lambda) = c_0(\lambda) - \sum_{n=1}^L a_n^4, \quad \ddot{c}_L(\lambda) = \ddot{c}_0(\lambda) - \sum_{\substack{n=1 \\ n: \text{even}}}^L a_n^4, \quad \text{and} \quad \dot{c}_L(\lambda) = \dot{c}_0(\lambda) - \sum_{\substack{n=1 \\ n: \text{odd}}}^L a_n^4.$$

The same applies to f_L and g_L .

References

- [1] Baldeaux, J., 2012. Exact simulation of the 3/2 model. *Int. J. Theor. Appl. Finance* 15, 1250032. doi:[10.1142/S021902491250032X](https://doi.org/10.1142/S021902491250032X).
- [2] Bernard, C., Cui, Z., 2014. Prices and asymptotics for discrete variance swaps. *Appl. Math. Finance* 21, 140–173. doi:[10.1080/1350486X.2013.820524](https://doi.org/10.1080/1350486X.2013.820524).
- [3] Broadie, M., Kaya, Ö., 2006. Exact simulation of stochastic volatility and other affine jump diffusion processes. *Oper. Res.* 54, 217–231. doi:[10.1287/opre.1050.0247](https://doi.org/10.1287/opre.1050.0247).
- [4] Cai, N., Song, Y., Chen, N., 2017. Exact simulation of the SABR model. *Oper. Res.* 65, 931–951. doi:[10.1287/opre.2017.1617](https://doi.org/10.1287/opre.2017.1617).
- [5] Choi, J., Kwok, Y.K., 2024. Simulation schemes for the Heston model with Poisson conditioning. *Eur. J. Oper. Res.* 314, 363–376. doi:[10.1016/j.ejor.2023.10.048](https://doi.org/10.1016/j.ejor.2023.10.048).
- [6] Choi, J., Liu, C., Seo, B.K., 2019. Hyperbolic normal stochastic volatility model. *J. Futur. Mark.* 39, 186–204. doi:[10.1002/fut.21967](https://doi.org/10.1002/fut.21967).
- [7] Cont, R., Da Fonseca, J., 2002. Dynamics of implied volatility surfaces. *Quant. Finance* 2, 45–60. doi:[10.1088/1469-7688/2/1/304](https://doi.org/10.1088/1469-7688/2/1/304).
- [8] Cui, Z., Kirkby, J.L., Nguyen, D., 2021. Efficient simulation of generalized SABR and stochastic local volatility models based on Markov chain approximations. *Eur. J. Oper. Res.* 290, 1046–1062. doi:[10.1016/j.ejor.2020.09.008](https://doi.org/10.1016/j.ejor.2020.09.008).
- [9] Daniluk, A., Muchorski, R., 2016. Approximations of bond and swaption prices In a Black–Karasiński model. *Int. J. Theor. Appl. Finance* 19, 1650017. doi:[10.1142/S0219024916500175](https://doi.org/10.1142/S0219024916500175), [arXiv:1506.00697](https://arxiv.org/abs/1506.00697).
- [10] Glasserman, P., Kim, K.K., 2011. Gamma expansion of the Heston stochastic volatility model. *Finance Stoch.* 15, 267–296. doi:[10.1007/s00780-009-0115-y](https://doi.org/10.1007/s00780-009-0115-y).
- [11] Heston, S.L., 1993. A closed-form solution for options with stochastic volatility with applications to bond and currency options. *Rev. Financ. Stud.* 6, 327–343. doi:[10.1093/rfs/6.2.327](https://doi.org/10.1093/rfs/6.2.327).
- [12] Kang, C., Kang, W., Lee, J.M., 2017. Exact simulation of the Wishart multidimensional stochastic volatility model. *Oper. Res.* 65, 1190–1206. doi:[10.1287/opre.2017.1636](https://doi.org/10.1287/opre.2017.1636).
- [13] Li, C., Wu, L., 2019. Exact simulation of the Ornstein–Uhlenbeck driven stochastic volatility model. *Eur. J. Oper. Res.* 275, 768–779. doi:[10.1016/j.ejor.2018.11.057](https://doi.org/10.1016/j.ejor.2018.11.057).
- [14] Loève, M., 1978. *Probability Theory II*. Number 46 in Graduate Texts in Mathematics. 4th ed ed., Berlin New York.
- [15] Schöbel, R., Zhu, J., 1999. Stochastic volatility with an Ornstein–Uhlenbeck process: An extension. *Rev. Finance* 3, 23–46. doi:[10.1023/A:1009803506170](https://doi.org/10.1023/A:1009803506170).
- [16] Scott, L.O., 1987. Option pricing when the variance changes randomly: Theory, estimation, and an application. *J. Financ. Quant. Anal.* 22, 419–438. doi:[10.2307/2330793](https://doi.org/10.2307/2330793).
- [17] Steele, J.M., 2001. *Stochastic Calculus and Financial Applications*. Number 45 in Applications of Mathematics. 4. print, [nachdr.] ed., New York, NY Berlin Heidelberg.
- [18] Stein, E.M., Stein, J.C., 1991. Stock price distributions with stochastic volatility: An analytic approach. *Rev. Financ. Stud.* 4, 727–752. doi:[10.1093/rfs/4.4.727](https://doi.org/10.1093/rfs/4.4.727).

- [19] Willard, G.A., 1997. Calculating prices and sensitivities for path-independent derivatives securities in multifactor models. *J. Deriv.* 5, 45–61. doi:[10.3905/jod.1997.407982](https://doi.org/10.3905/jod.1997.407982).